

# Isolation of High-Affinity Peptide Antagonists of 14-3-3 Proteins by Phage Display<sup>†</sup>

Bingcheng Wang,<sup>\*,‡</sup> Hongzhu Yang,<sup>§,||</sup> Yun-Cai Liu,<sup>⊥</sup> Tomas Jelinek,<sup>@</sup> Lixin Zhang,<sup>§,§</sup> Erkki Ruoslahti,<sup>#</sup> and Haian Fu<sup>\*,§</sup>

*Rammelkamp Center for Research, Case Western Reserve University, Cleveland, Ohio 44109, Department of Pharmacology and Graduate Program in Biochemistry, Cell, and Developmental Biology, Emory University, Atlanta, Georgia 30322, La Jolla Institute for Allergy and Immunology, San Diego, California 92121, Department of Microbiology and Cancer Center, University of Virginia, Charlottesville, Virginia 22908, and Burnham Institute, La Jolla, California 92037*

*Received June 14, 1999; Revised Manuscript Received July 22, 1999*

**ABSTRACT:** The 14-3-3 proteins interact with diverse cellular molecules involved in various signal transduction pathways controlling cell proliferation, transformation, and apoptosis. To aid our investigation of the biological function of 14-3-3 proteins, we have set out to identify high-affinity antagonists. By screening phage display libraries, we have identified a set of peptides which bind 14-3-3 proteins. One of these peptides, termed R18, exhibited a high affinity for different isoforms of 14-3-3 with estimated  $K_D$  values of  $7-9 \times 10^{-8}$  M. Recognition of multiple isoforms of 14-3-3 suggests the targeting of R18 to a structure that is common among 14-3-3 proteins, such as the conserved ligand-binding groove. Indeed, mutations that alter critical residues in the ligand-binding site of 14-3-3 drastically decreased the level of 14-3-3–R18 association. R18 efficiently blocked the binding of 14-3-3 to the kinase Raf-1, a physiological ligand of 14-3-3, and effectively abolished the protective role of 14-3-3 against phosphatase-induced inactivation of Raf-1. The cocrystal structure of R18 in complex with 14-3-3 $\zeta$  revealed the occupancy of the general binding groove of 14-3-3 $\zeta$  by R18, explaining the potent inhibitory effect of R18 on 14-3-3–ligand interactions. Such a well-defined peptide will be an effective tool for probing the role of 14-3-3 in various signaling pathways, and may lead to the development of 14-3-3 antagonists with pharmacological applications.

The 14-3-3 proteins are highly conserved, dimeric molecules found in all eukaryotic organisms (see refs 1–3 for reviews). The 14-3-3 family consists of at least seven isoforms in mammalian cells ( $\beta$ ,  $\epsilon$ ,  $\gamma$ ,  $\eta$ ,  $\sigma$ ,  $\tau$ , and  $\zeta$ ). Although the biochemical function of 14-3-3 remains largely unclear, 14-3-3 has been found to interact with critical regulatory proteins controlling a wide array of signaling pathways. These 14-3-3 interacting proteins include Raf-1 (4–9), phosphatidylinositol 3-kinase (10), Cdc25 (11), the tumor suppressor p53 (12), and a proapoptotic member of the Bcl-2 family, Bad (13). Through interaction with critical regulatory proteins, 14-3-3 proteins play a pivotal role in regulating diverse biological processes, such as the control

of cell cycle checkpoints (11, 14–17), survival signaling (13, 18–20), and viral and bacterial pathogenesis (21–24).

Many 14-3-3–ligand interactions are phosphorylation-dependent (25, 26). Phosphoserine-containing motifs have been identified in Raf-1 and other 14-3-3 ligands that serve as critical structural determinants of 14-3-3 association (27, 28). For coordinating the interaction with the phosphate group, 14-3-3 proteins employ a cluster of basic residues in a conserved ligand-binding site that includes Lys-49, Arg-56, and Arg-127. This model was initially based on the crystal structure of 14-3-3 $\zeta$  (29), and now both mutational analysis and structural studies have confirmed this phosphoserine-binding site of 14-3-3 (28, 30–33). Interestingly, this phosphoserine recognition site is also involved in the binding of nonphosphorylated exoenzyme S of *Pseudomonas aeruginosa* (30, 34, 48). Thus, the isolation of small molecules that bind in this conserved ligand binding site of 14-3-3 may provide general 14-3-3 antagonists.

To identify 14-3-3 antagonists, we have used random peptide phage display technology (35). Here we report the isolation and characterization of a high-affinity nonphosphorylated peptide ligand for 14-3-3 proteins. This peptide, R18, bound 14-3-3 proteins without isoform selectivity, inhibited the interaction of 14-3-3 with the physiological substrate Raf-1, and diminished the protective role of 14-3-3 against phosphatase-induced Raf-1 inactivation. R18 represents a potentially useful tool for the dissection of the biological function of 14-3-3.

<sup>†</sup> This work was supported by NIH Grants DK54178 to B.W., CA 28896 to E.R., and GM53165 to H.F.; by Department of Army Grant PC970263 and American Heart Association Northeast Ohio Affiliate Grant 9806275 to B.W.; and by California Tobacco-Related Disease Grant 4IT0147 and Cancer Center Support Grant CA30199 to E.R. H.F. is a recipient of the Burroughs Wellcome Fund New Investigator Award.

\* Corresponding authors. Phone: (404) 727-0368. Fax: (404) 727-0365. E-mail: hfu@pharm.emory.edu.

<sup>‡</sup> Case Western Reserve University.

<sup>§</sup> Department of Pharmacology, Emory University.

<sup>||</sup> Graduate Program in Biochemistry, Cell, and Developmental Biology, Emory University.

<sup>⊥</sup> La Jolla Institute for Allergy and Immunology.

<sup>@</sup> University of Virginia.

<sup>§</sup> Current address: Microbia Inc., Cambridge, MA 02139.

<sup>#</sup> Burnham Institute.

## MATERIALS AND METHODS

**Materials.** The fUSE5 virion (35) and *Escherichia coli* strains K91kan, K802, and MC1061 were gifts from G. Smith (Washington University, St. Louis, MO). Glutathione *S*-transferase (GST<sup>1</sup>)–14-3-3 $\tau$  and GST–14-3-3 $\zeta$  were expressed and purified as described previously (10, 24). GST–14-3-3 $\beta$  was a gift from S. Li (Yale University, New Haven, CT). Baculoviruses expressing  $\beta$ -gal and Raf-1 were gifts from U. Rapp (University of Wurzburg, Wurzburg, Germany). Rabbit polyclonal antibodies against Raf-1, 14-3-3 $\beta$ , and 14-3-3 $\zeta$  were from Santa Cruz Biotechnology (Santa Cruz, CA). The R18 peptide was generated on an Applied Biosystem model 430A synthesizer by standard Merrifield solid phase synthesis protocols and *tert*-butoxycarbonyl chemistry.

**Selection of 14-3-3-Binding Phage.** Two libraries displaying X<sub>2</sub>CX<sub>14</sub>CX<sub>2</sub> and X<sub>2</sub>CX<sub>18</sub> random peptides (X being any amino acid and C being cysteine) were constructed essentially as described previously (36–38). Biopanning on GST–14-3-3 $\tau$  was carried out as reported previously (37–39). Briefly, a microtiter well was coated overnight with 200  $\mu$ L of 10  $\mu$ g/mL GST–14-3-3 $\tau$  in TBS [50 mM Tris-HCl (pH 7.5) and 150 mM NaCl] and blocked with 1% BSA. About  $2 \times 10^{11}$  transducing units of phage from each library was combined and incubated with the coated well overnight at 4 °C in 200  $\mu$ L of TBS containing 1% BSA and 1 mM MgCl<sub>2</sub>. The well was washed 10 times with TBS and eluted with 0.1 M glycine (pH 2.2). DNA from individual phage clones was sequenced after three rounds of selection as described previously (39).

**Production of GST Fusion Peptides.** Two oligonucleotides complementary to constant regions surrounding the insertion site in fUSE5 were synthesized (5' primer, 5'-AGGCTC-GAGGATCCTCGGCCGACGGGGCT-3'; and 3' primer, 5'-AGGTCTAGAATTCGCCCCAGCGGCCCC-3'). Peptide coding sequences from individual phage clones were cloned into pGEX-2T following PCR amplification using the two primers. GST fusion peptides were purified as described previously (36). To obtain the R18 peptide, GST–R18 was cleaved using thrombin at a concentration of 0.5  $\mu$ g/mg of fusion peptide.

**Solid Phase Binding Assay.** Ten micrograms of protein in 0.1 mL of 50 mM potassium phosphate buffer (pH 7.5) was iodinated using Iodo-Gen source (40). Typically, a specific activity of  $5 \times 10^8$  mCi/mmol was obtained. Solid phase binding assays were carried out on Immulon 2 Removawell strips (Dynex Technologies). GST fusion proteins were immobilized onto wells in TBS overnight at 4 °C, and nonspecific binding sites were blocked with 400  $\mu$ L of 1% BSA in TBS for 2 h at room temperature. In a typical assay, 500 000 cpm of <sup>125</sup>I-labeled protein in 50  $\mu$ L of binding buffer (TBS with 1% BSA and 1 mM MgCl<sub>2</sub>) was added to each well. After incubation for 3 h at room temperature, the wells were washed four times with TBS and bound proteins

were quantified on a  $\gamma$ -counter. To measure the dissociation constant, a fixed amount of the radiolabeled proteins was mixed with serial dilutions of the unlabeled proteins. For monitoring the interaction of R18 with the 14-3-3 $\zeta$  mutant K49E and V176D, GST–R18 immobilized on glutathione beads was mixed with either WT or mutant proteins. The 14-3-3 proteins in complex with GST–R18 were isolated after extensive washing, resolved on SDS–PAGE (12.5%), and revealed by immunoblotting with anti-14-3-3 antiserum using ECL (Amersham Pharmacia Biotech).

**Protein Overlay Assay.** Sf9 insect cells were infected with recombinant baculoviruses expressing  $\beta$ -gal or Raf-1 at an estimated multiplicity of infection of 10. Cells were lysed 48 h later with lysis buffer containing 1% Triton X-100, 10% glycerol, 2 mM EDTA, 137 mM NaCl, 20 mM Tris-HCl (pH 8.0), 1 mM phenylmethanesulfonyl fluoride, aprotinin (1  $\mu$ g/mL), and leupeptin (2  $\mu$ g/mL). Raf-1 was purified from the cell lysate using an immunoaffinity column coupled with a rabbit polyclonal antibody against the last 12 amino acids of Raf-1. Purified Raf-1 was separated by SDS–PAGE and blotted onto an Immobilon-P membrane (Millipore). Membrane strips were blocked for 2 h with 5% nonfat milk in TBS and equilibrated for 1 h with K50 binding buffer containing 20 mM HEPES (pH 7.6), 50 mM KCl, 2.5 mM MgCl<sub>2</sub>, 0.1% Triton X-100, 2 mM EDTA, and 1% nonfat milk. For binding reactions, filter strips were incubated with  $1 \times 10^6$  cpm of <sup>125</sup>I-labeled GST–14-3-3 $\tau$ /mL in K50 buffer for 4 h at 4 °C. The strips were washed five times with TBS and 0.1% Tween 20 and exposed to X-ray film overnight at –80 °C.

**Assays of Raf-1 Kinase Activity.** GST–Ras was conjugated to *N*-hydroxysuccinimide-derivatized silica beads (Affinity Technology) and loaded with a nonhydrolyzable analogue of GTP, GMP-PNP. Sf9 cells were coinfecting with baculoviruses expressing Raf-1, Src(Y527F), and H-Ras and lysed in p21 buffer [20 mM MOPS (pH 8.0), 200 mM sucrose, 1 mM MgCl<sub>2</sub>, 1 mM DTT, and 1 mM sodium vanadate] (41). Lysates were incubated with GST–Ras–GMP-PNP on silica beads at 4 °C for 1 h to bind Raf-1. The beads were washed twice in p21 buffer containing 0.5% CHAPS and 0.5% Triton X-100, and then twice with p21 buffer and 0.5% sodium deoxycholate. Finally, the beads were washed in kinase buffer [50 mM HEPES (pH 7.5), 50 mM NaCl, 10 mM MgCl<sub>2</sub>, and 1 mM DTT] and used for the kinase assay (41) with 200 ng of recombinant His-tagged MEK-1 per sample, 2  $\mu$ g of kinase inactive Erk2 per sample (K52R), 100  $\mu$ M ATP, and [ $\gamma$ -<sup>32</sup>P]ATP (2500 cpm/pmol) at 30 °C for 10 min. Reactions were terminated by the addition of SDS sample buffer.

To inactivate Raf-1 with PTP-1B prior to using it in kinase assays, Raf-1 bound to Ras–GMP-PNP–silica beads was washed with p21 buffer and detergents as described above, and then twice in phosphatase buffer [25 mM Tris-HCl (pH 7.6), 10% glycerol, 1 mM DTT, 0.1 mM EDTA, and 0.01% Nonidet P-40]. The beads were incubated with 0.5  $\mu$ g of GST–PTP-1B in phosphatase buffer for 30 min at 37 °C. In the indicated samples, 1  $\mu$ g of 14-3-3 that was untreated or treated with 5  $\mu$ g of GST–R18 for 15 min at 4 °C was added to Raf-1 prior to the addition of PTP-1B. Samples were mixed, incubated at 35 °C for 30 min, and subjected to kinase activity assays as described above.

<sup>1</sup> Abbreviations: BSA, bovine serum albumin; GST, glutathione *S*-transferase; TBS, Tris-buffered saline; DTT, dithiothreitol; Erk, extracellular signal-regulated kinase or mitogen-activated protein kinase (MAPK); MEK, MAPK/Erk kinase; PTP-1B, protein tyrosine phosphatase 1B; PAGE, polyacrylamide gel electrophoresis.

Table 1: Isolation of 14-3-3τ-Binding Peptides Displayed on Phage<sup>a</sup>

clone	amino acid sequence	library	frequency	phage attachment (OD <sub>590</sub> )
R18	PHCVPRDLS <b>WLDL</b> LEANMCLP	X <sub>2</sub> CX <sub>14</sub> CX <sub>2</sub>	18	0.718
C43	VTCSIAEY <b>GWLDL</b> AAACSS	X <sub>2</sub> CX <sub>14</sub> CX <sub>2</sub>	1	0.339
C12	PRCMTSYWMDGLQPESCKG	X <sub>2</sub> CX <sub>14</sub> CX <sub>2</sub>	1	0.369
C48	RNCWGNIPLTSSSVRLCDAR	X <sub>2</sub> CX <sub>18</sub>	1	0.156
CO3	RVCAAPESRLFRGMPLGCDD	X <sub>2</sub> CX <sub>14</sub> CX <sub>2</sub>	1	0.135
C05	DACSKQGMGVLLSGWPGPCTT	X <sub>2</sub> CX <sub>18</sub>	1	0.152
C06	PACLL <b>RSE</b> EYVVECGGDVGLE	X <sub>2</sub> CX <sub>18</sub>	1	0.137
C07	VCCGVNESLS <b>RS</b> AHAD <b>S</b> ALMR	X <sub>2</sub> CX <sub>18</sub>	1	0.104
C41	EVCHMPVSCGP <b>TER</b> SLGGESL	X <sub>2</sub> CX <sub>18</sub>	1	0.121
C02	DNLKTLLASKWFHETAKGW	mutant	1	0.130
C01	RFTTQGERGITHLRESSTL	mutant	1	0.067
C15	SRCRLEYAWACGW	mutant	1	0.506

<sup>a</sup> For the phage attachment assay, microtiter wells were coated with 1 μg/mL GST–14-3-3τ and incubated with phage from individual clones. Bound phage was used to infect bacteria, and the OD<sub>590</sub> after overnight culture at room temperature reflects the input phage titer (37).

## RESULTS

**Isolation of Peptide Ligands for 14-3-3τ.** To identify peptide ligands for 14-3-3 proteins, we screened two phage libraries displaying 20-mer (X<sub>2</sub>CX<sub>14</sub>CX<sub>2</sub>) and 21-mer (X<sub>2</sub>-CX<sub>18</sub>) random peptides, and obtained a set of phage-displayed peptides that bind GST–14-3-3τ (Table 1). After three rounds of panning, a majority of isolated phages (18 of 29) contained the same sequence from the 20-mer library (PHCVPRDLS**WLDL**LEANMCLP, named R18), suggesting that this screening process was approaching saturation. Examination of the isolated peptide sequences revealed a tetrapeptide motif, **WLDL**, located in the middle of the R18 peptide. Sequences identical or similar to the **WLDL** motif also occurred in clones C43, C12, and C48. Three of the clones that we identified appear to be mutants because their sequences could not have been derived directly from either library (Table 1). It is also interesting to note that three of the selected clones (C06, C07, and C41) contain sequences partially resembling the prototype phosphoserine motif of many 14-3-3 ligands, **RSXpSXP** (italicized and underlined in Table 1; 27, 28). These peptides have an **RSX**<sub>(1–3)</sub>**E/D**-like motif where the negatively charged Glu or Asp may partially mimic phosphoserine for 14-3-3 binding.

To select clones for further analysis, we determined the relative affinities of individual phage clones for 14-3-3 using a phage attachment assay essentially as previously described (37). Clone R18, which occurred most frequently, had the highest relative affinity, followed by that of clone C15; the remaining clones exhibited lower levels of binding (Table 1). On the basis of these results, inserts from the three clones with the highest affinities (R18, C15, and C12) were subcloned into a bacterial expression vector as GST fusion proteins. Consistent with the phage attachment assay, <sup>125</sup>I-labeled GST–R18 fusion peptide bound avidly to 14-3-3τ in a solid phase binding assay; more than 20% of the input probe was captured (Figure 1). GST–C15 and GST–C12 bound much less well, but clearly above the background seen with GST alone (Figure 1, inset). Thus, R18 represents a high-affinity ligand of 14-3-3τ and was characterized in detail.

**R18 Is Specific for 14-3-3 Proteins without Isoform Selectivity.** To determine the specificity of peptide R18 for 14-3-3 proteins, we examined the binding of R18 to proteins from total lysates of NIH 3T3 cells. For this experiment,

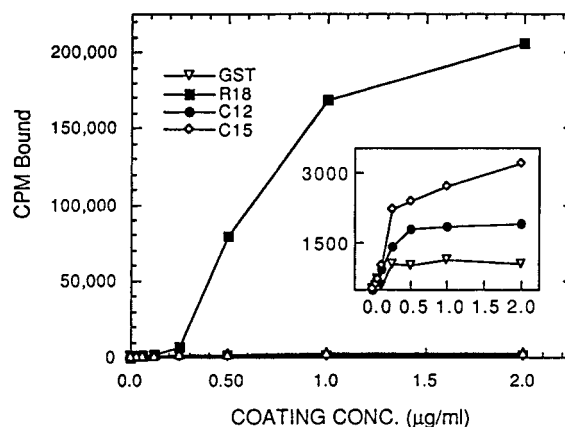


FIGURE 1: Binding of recombinant peptides to 14-3-3τ. GST-tagged peptides were labeled with <sup>125</sup>I and tested for binding to 14-3-3τ immobilized on microtiter wells. After incubation for 3 h, the wells were washed with TBS and bound peptides were quantified with a γ-counter. The inset represents an expanded version of the same plot showing the binding of low-affinity clones (C12 and C15) and the GST control. Values are means from duplicate wells with less than 10% variation.

total proteins of NIH 3T3 cells were metabolically labeled with [<sup>35</sup>S]methionine, and incubated with GST–R18 immobilized on glutathione–Sephadex beads. After extensive washing and separation by SDS–PAGE, proteins bound to GST–R18 were identified by autoradiography (Figure 2A). We found that GST–R18 specifically pulled down a major band of proteins around 30 kDa, which is similar in size to 14-3-3 proteins. Immunoblotting with a polyclonal 14-3-3 antibody revealed that this band contained 14-3-3 proteins (Figure 2B) and that the GST control protein was unable to pull down this band. Thus, R18 specifically associates with 14-3-3 proteins despite the presence of many other proteins in total cell lysates.

The family of 14-3-3 proteins exists in multiple isoforms in mammalian cells. R18 was initially isolated for its binding to 14-3-3τ. To test whether R18 is specific for the τ isoform or general for the family of 14-3-3 proteins, we analyzed the binding of R18 to two other isoforms, β and ζ, in addition to the binding to τ in a solid phase binding assay. All three isoforms of 14-3-3 that were tested avidly bound to GST–R18, but not to the GST control (Figure 3A). Scatchard analysis showed that each isoform that was tested exhibited similar affinities for the R18 peptide with *K<sub>D</sub>* values of around 7–9 × 10<sup>−8</sup> M (Figure 3B–D). The binding of all



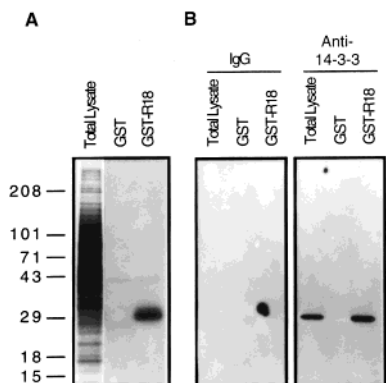


FIGURE 2: R18 peptide specifically binds cellular 14-3-3 proteins. (A) NIH 3T3 cells were metabolically labeled with [ $^{35}$ S]methionine. Lysates were incubated with immobilized GST-R18 or GST (10  $\mu$ g). After being washed with lysis buffer, bound materials were eluted with 5 mM glutathione, resolved by SDS-PAGE, and exposed to X-ray film. (B) Unlabeled cells were processed in the same fashion as described for panel A. The GST-R18-associated proteins were separated by SDS-PAGE, transferred to Immobilon-P membranes, and blotted with normal rabbit IgG or anti-14-3-3 serum as indicated.

three isoforms fit a one-binding site model, suggesting that the two binding sites on a 14-3-3 dimer are equivalent and may function independently of one another. Because three different isoforms of 14-3-3 interact with R18 with similar affinities, these data suggest that a structure conserved among 14-3-3 isoforms may mediate the binding of R18.

**Mutations in the Conserved Amphipathic Groove of 14-3-3 Disrupt Its Binding to R18.** From crystal structure analysis, an amphipathic groove in 14-3-3 $\zeta$  was proposed to be the primary ligand-binding site (29). The surface residues lining this binding groove are conserved among 14-3-3 isoforms (29, 42). To determine whether R18 specifically

targets this ligand-binding site, we examined the effect of defined mutations of 14-3-3 $\zeta$ , K49E and V176D, on the binding of R18 to 14-3-3 $\zeta$ . Lys-49 is located in the conserved ligand-binding site, forming a critical part of a basic cluster that interacts with the phosphate group in phosphoserine-containing ligands (28, 29). Val-176 is also located in this groove on the hydrophobic side. Mutations of Lys-49 and Val-176 have been shown to disrupt the interaction of 14-3-3 $\zeta$  with Raf-1 and other natural ligands (30, 31, 43). As shown in Figure 4, R18 bound effectively to WT 14-3-3 $\zeta$ , but bound with a greatly decreased affinity to the charge-reversal mutant of Lys-49, K49E, and the hydrophobic residue mutant V176D. It is likely that R18 binds 14-3-3 $\zeta$  through this general ligand-binding groove, and thus may be able to antagonize the interaction of 14-3-3 with its natural ligands.

**R18 Blocks the Binding of 14-3-3 to Raf-1.** The targeting of R18 to the conserved ligand binding site of 14-3-3 predicts that R18 may serve as a competitive inhibitor of 14-3-3–ligand interactions. To test this idea, we examined the effect of R18 on the interaction of 14-3-3 with Raf-1. Raf-1 is a critical component of growth factor-mediated signal transduction pathways (44). It has been well established that 14-3-3 specifically interacts with Raf-1 and plays an important role in Raf-1-mediated signal transduction (1–3, 33, 45, and references therein). In agreement with previous reports, 14-3-3 $\tau$  effectively bound to Raf-1 in a filter binding assay (Figure 5). Importantly, pretreatment of 14-3-3 $\tau$  with GST-R18 at a concentration as low as 5 nM greatly reduced the level of binding of 14-3-3 $\tau$  to Raf-1, while GST alone showed no inhibitory effect. The inhibition caused by the fusion peptide was not due to steric hindrance of the GST fusion partner because the R18 peptide cleaved from the GST fusion (Figure 5, lanes 6–8) and the synthetic R18 peptide

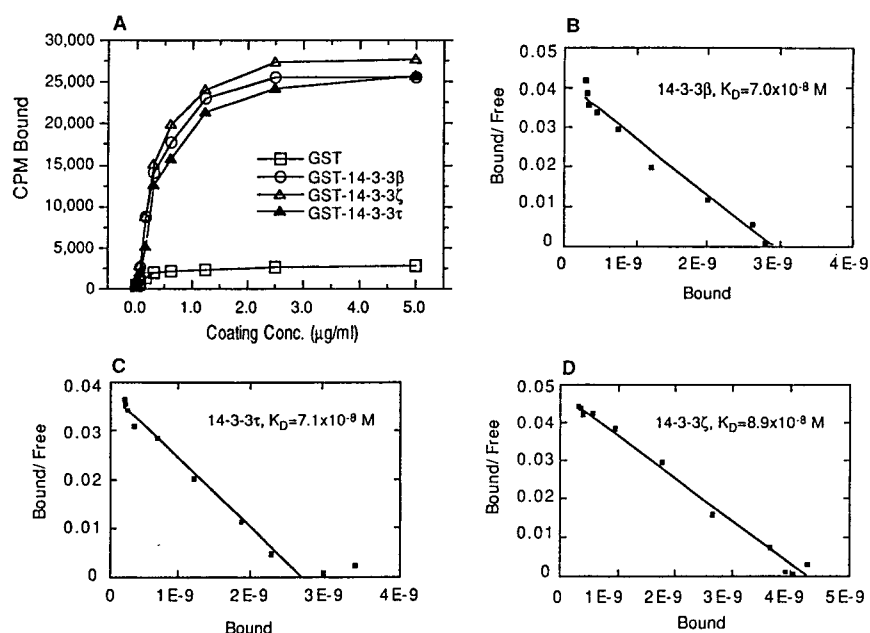


FIGURE 3: R18 peptide binds equally well to several isoforms of 14-3-3. (A) Three 14-3-3 isoforms ( $\beta$ ,  $\tau$ , and  $\tau$ ) were expressed in *E. coli* as GST fusion proteins and labeled with  $^{125}$ I, and about  $1 \times 10^6$  cpm of labeled proteins was added to each well in Removawell strips that had been coated with serially diluted GST-R18 peptide. After extensive washing, bound 14-3-3 proteins were quantified (CPM Bound). (B–D) Wells were coated with 1  $\mu$ g/mL GST-R18 peptide.  $^{125}$ I-labeled 14-3-3 proteins were allowed to bind to the wells in the presence of serially diluted unlabeled 14-3-3 starting with a 500-fold molar excess. Analysis of binding, including model fitting, saturation, and Scatchard curve construction, was performed with the Ligand program (46). Each data point represents the mean from duplicate wells with variation of less than 10%.

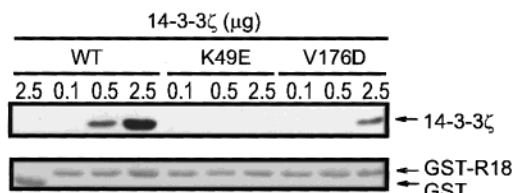


FIGURE 4: Mutations of Lys-49 and Val-176 in the ligand-binding groove of 14-3-3ζ disrupt its interaction with R18. Immobilized GST-R18 or GST (lower panel) was incubated with WT or mutant 14-3-3ζ (K49E and V176D) proteins. After washing, 14-3-3ζ bound to GST-R18 or GST was revealed by immunoblotting using anti-14-3-3 serum (upper panel).

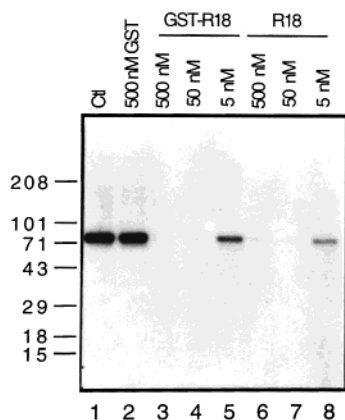


FIGURE 5: Raf-1 association with 14-3-3 is disrupted by the R18 peptide. Sf9 cells expressing human Raf-1 were lysed. Raf-1 was isolated using an immunoaffinity column, separated by SDS-PAGE, and transferred to a nylon membrane. Filter strips were incubated with  $^{125}$ I-labeled 14-3-3τ that was untreated (Ct), treated with GST, or treated with the indicated concentrations of either GST-R18 or R18 cleaved from GST-R18. After washing, 14-3-3τ bound to Raf-1 was identified by autoradiography.

(data not shown) were as effective as GST-R18 in inhibiting 14-3-3 binding to Raf-1. R18 appears to be a potent inhibitor of the interaction of 14-3-3 with its physiological ligand Raf-1.

**R18 Inhibits the Protective Role of 14-3-3 against Phosphatase-Induced Inactivation of Raf-1.** Dent et al. (41) demonstrated that the kinase activity of Raf-1 purified from Sf9 cells is susceptible to inactivation by protein phosphatases such as PTP-1B. Interestingly, 14-3-3 proteins can protect Raf-1 from inactivation by phosphatases in vitro (41). We have adapted this system to address the functional significance of inhibition of the association between 14-3-3 and Raf-1 by R18 (Figure 6). In agreement with previous reports (41), activated Raf-1 phosphorylated its physiological substrate MEK-1, and indirectly activated the downstream substrate of MEK-1, Erk2 (Figure 6). The kinase activity of Raf-1 was greatly reduced by treatment of Raf-1 with PTP-1B (lane 4). Addition of 14-3-3ζ or the phosphatase inhibitor vanadate to the Raf-1 preparation before PTP-1B treatment prevented Raf-1 inactivation (lanes 3 and 5), suggesting that 14-3-3 binds to the phosphorylated Raf-1 and prevents its inactivation by PTP-1B. However, when 14-3-3ζ was incubated with GST-R18 prior to addition to the Raf-1 reaction mixture, it was no longer able to prevent Raf-1 inactivation by PTP-1B, whereas incubation with GST alone did not have any effect (Figure 6, compare lanes 6 and 8). Thus, the R18 peptide can also block a functional effect of 14-3-3 association with Raf-1.

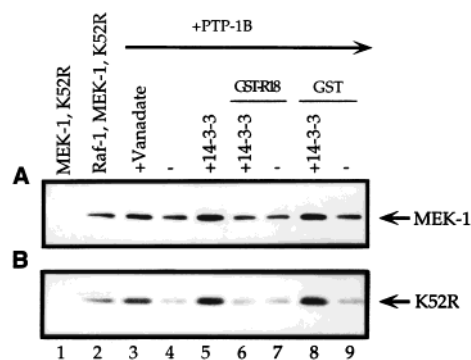


FIGURE 6: R18 inhibits the protective role of 14-3-3 against PTP-1B-induced Raf-1 inactivation. Active Raf-1 was purified on GST-Ras-GMP-PNP covalently linked to silica beads from Sf9 cells coexpressing H-Ras. Where indicated, approximately 10 ng of Raf-1 was mixed with 14-3-3ζ (1 μg) alone or 14-3-3ζ that was preincubated with 5 μg of either GST-R18 or GST. In lane 3, 1 mM sodium orthovanadate was used. Both 14-3-3-treated and untreated Raf-1 were incubated with PTP-1B (1 μg). Raf-1 kinase activities were then measured by adding MEK-1 (0.2 μg) and kinase inactive Erk2 (K52R; 2 μg) in the presence of  $[\gamma\text{-}^{32}\text{P}]\text{ATP}$ . The reactions were stopped by SDS sample buffer, and the mixtures were separated by SDS-PAGE and detected using a Phosphor-Imager.

## DISCUSSION

We have isolated the high-affinity 14-3-3 antagonist R18 from a library displaying random peptides. This peptide bound specifically to multiple isoforms of purified 14-3-3 proteins and was found to interact with only a single band of proteins from total cell lysates. Functionally, the R18 peptide blocked the association of 14-3-3 with Raf-1, and rendered 14-3-3 unable to protect Raf-1 against inactivation by phosphatases. R18 may serve as a general inhibitor of 14-3-3-ligand interactions.

The potent inhibitory effect of R18 on 14-3-3-ligand interactions can be explained by the localization of R18 in the conserved amphipathic groove of 14-3-3, a site that mediates its interaction with diverse natural ligands (28, 29, 32, 42). In the cocrystal structure of 14-3-3ζ in complex with R18, the pentapeptide WLDLE, which contains the tetrapeptide motif (WLDL) identified by phage display, occupies the phosphoserine recognition site in the groove (32). Acidic residues of the pentapeptide (Asp and Glu) mimic the phosphate group of phosphoserine-containing ligands and are placed next to a cluster of basic residues of 14-3-3ζ (Lys-49, Arg-56, Arg-60, and Arg-127). Consistent with this model, a charge-reversal mutation of 14-3-3ζ, K49E, drastically decreased the level of binding of 14-3-3ζ to R18. A mutation in the hydrophobic face of the groove, V176D, which disrupts 14-3-3-Raf-1 binding, also decreased the extent of the 14-3-3ζ-R18 interaction (Figure 4). Competition between R18 and Raf-1 for the same set of residues in the binding groove of 14-3-3 may account for the inhibitory effect of R18 on the 14-3-3-Raf-1 interaction (Figures 5 and 6). Because residues lining the amphipathic groove of 14-3-3ζ, including the basic cluster, are conserved among all mammalian isoforms of 14-3-3, it is expected that R18 can bind to different isoforms with similar affinities. Similar dissociation constants for R18 among the β, τ, and ζ isoforms support this notion.

<sup>2</sup> S. C. Masters, H. Yang, and H. Fu, unpublished results.

The conserved amphipathic groove that binds R18 is also involved in binding to diverse protein ligands. It is possible that R18 can block the interaction of 14-3-3 with most or all of its ligands. Indeed, we have shown that R18 effectively inhibited the interaction of 14-3-3 $\zeta$  with phosphorylated Bad and ASK1 (apoptosis signal-regulating kinase 1), and unphosphorylated exoenzyme S, in addition to Raf-1 (34, 47, 48).<sup>2</sup> Therefore, R18 may be a general antagonist of 14-3-3 proteins, which can be expressed in cells to probe the role of 14-3-3 in diverse signaling pathways.

Although the pentapeptide WLDLE contacts the amphipathic groove of 14-3-3 $\zeta$  in an amphipathic conformation, it should be emphasized that the WLDLE motif alone is not sufficient for high-affinity binding. A peptide containing only the WLDLE sequence showed no detectable binding to 14-3-3.<sup>2</sup> Therefore, residues outside the WLDLE motif are likely to contribute to the binding affinity and specificity of R18 for 14-3-3.

In conclusion, we have isolated a peptide that targets a general ligand-binding site on 14-3-3 proteins. The relative simplicity of R18 and extended stability of the R18–14-3-3 complex will prove to be valuable in probing the function of 14-3-3 proteins.

## ACKNOWLEDGMENT

We thank Shane Masters for critical reading of the manuscript and assistance in the preparation of the figures.

## REFERENCES

- Aitken, A. (1996) *Trends Cell Biol.* 6, 341–7.
- Reuther, G. W., and Pendergast, A. M. (1996) *Vitam. and Horm. (San Diego)* 52, 149–75.
- Morrison, D. (1994) *Science* 266, 56–7.
- Fantl, W. J., Muslin, A. J., Kikuchi, A., Martin, J. A., MacNicol, A. M., Gross, R. W., and Williams, L. T. (1994) *Nature* 371, 612–4.
- Freed, E., Symons, M., Macdonald, S. G., McCormick, F., and Ruggieri, R. (1994) *Science* 265, 1713–6.
- Fu, H., Xia, K., Pallas, D. C., Cui, C., Conroy, K., Narsimhan, R. P., Mamon, H., Collier, R. J., and Roberts, T. M. (1994) *Science* 266, 126–9.
- Irie, K., Gotoh, Y., Yashar, B. M., Errede, B., Nishida, E., and Matsumoto, K. (1994) *Science* 265, 1716–9.
- Li, S., Janosch, P., Tanji, M., Rosenfeld, G. C., Waymire, J. C., Mischak, H., Kolch, W., and Sedivy, J. M. (1995) *EMBO J.* 14, 685–96.
- Luo, Z. J., Zhang, X. F., Rapp, U., and Avruch, J. (1995) *J. Biol. Chem.* 270, 23681–7.
- Bonnefoy-Berard, N., Liu, Y. C., von Willebrand, M., Sung, A., Elly, C., Mustelin, T., Yoshida, H., Ishizaka, K., and Altman, A. (1995) *Proc. Natl. Acad. Sci. U.S.A.* 92, 10142–6.
- Conklin, D. S., Galaktionov, K., and Beach, D. (1995) *Proc. Natl. Acad. Sci. U.S.A.* 92, 7892–6.
- Waterman, M. J., Stavridi, E. S., Waterman, J. L., and Halazonetis, T. D. (1998) *Nat. Genet.* 19, 175–8.
- Zha, J., Harada, H., Yang, E., Jockel, J., and Korsmeyer, S. J. (1996) *Cell* 87, 619–28.
- Kumagai, A., Yakowec, P. S., and Dunphy, W. G. (1998) *Mol. Biol. Cell* 9, 345–54.
- Lopez-Girona, A., Furnari, B., Mondesert, O., and Russell, P. (1999) *Nature* 397, 172–5.
- Peng, C. Y., Graves, P. R., Thoma, R. S., Wu, Z., Shaw, A. S., and Piwnica-Worms, H. (1997) *Science* 277, 1501–5.
- Hermeking, H., Lengauer, C., Polyak, K., He, T. C., Zhang, L., Thiagalingam, S., Kinzler, K. W., and Vogelstein, B. (1997) *Mol. Cell* 1, 3–11.
- Datta, S. R., Dudek, H., Tao, X., Masters, S., Fu, H., Gotoh, Y., and Greenberg, M. E. (1997) *Cell* 91, 231–41.
- del Peso, L., Gonzalez-Garcia, M., Page, C., Herrera, R., and Nunez, G. (1997) *Science* 278, 687–9.
- Hsu, S. Y., Kaipia, A., Zhu, L., and Hsueh, A. J. (1997) *Mol. Endocrinol.* 11, 1858–67.
- Pallas, D. C., Fu, H., Haehnel, L. C., Weller, W., Collier, R. J., and Roberts, T. M. (1994) *Science* 265, 535–7.
- Reuther, G. W., Fu, H., Cripe, L. D., Collier, R. J., and Pendergast, A. M. (1994) *Science* 266, 129–33.
- Cullere, X., Rose, P., Thathamangalam, U., Chatterjee, A., Mullane, K. P., Pallas, D. C., Benjamin, T. L., Roberts, T. M., and Schaffhausen, B. S. (1998) *J. Virol.* 72, 558–63.
- Fu, H., Coburn, J., and Collier, R. J. (1993) *Proc. Natl. Acad. Sci. U.S.A.* 90, 2320–4.
- Furukawa, Y., Ikuta, N., Omata, S., Yamauchi, T., Isobe, T., and Ichimura, T. (1993) *Biochem. Biophys. Res. Commun.* 194, 144–9.
- Michaud, N. R., Fabian, J. R., Mathes, K. D., and Morrison, D. K. (1995) *Mol. Cell. Biol.* 15, 3390–7.
- Muslin, A. J., Tanner, J. W., Allen, P. M., and Shaw, A. S. (1996) *Cell* 84, 889–97.
- Yaffe, M. B., Rittinger, K., Volinia, S., Caron, P. R., Aitken, A., Leffers, H., Gamblin, S. J., Smerdon, S. J., and Cantley, L. C. (1997) *Cell* 91, 961–71.
- Liu, D., Bienkowska, J., Petosa, C., Collier, R. J., Fu, H., and Liddington, R. (1995) *Nature* 376, 191–4.
- Zhang, L., Wang, H., Liu, D., Liddington, R., and Fu, H. (1997) *J. Biol. Chem.* 272, 13717–24.
- Wang, H., Zhang, L., Liddington, R., and Fu, H. (1998) *J. Biol. Chem.* 273, 16297–304.
- Petosa, C., Masters, S. C., Bankston, L. A., Pohl, J., Wang, B., Fu, H., and Liddington, R. C. (1998) *J. Biol. Chem.* 273, 16305–10.
- Thorson, J. A., Yu, L. W. K., Hsu, A. L., Shih, N. Y., Graves, P. R., Tanner, J. W., Allen, P. M., Piwnica-Worms, H., and Shaw, A. S. (1998) *Mol. Cell. Biol.* 18, 5229–38.
- Masters, S. C., Pederson, K. J., Zhang, L., Barbieri, J. T., and Fu, H. (1999) *Biochemistry* 38, 5216–21.
- Scott, J. K., and Smith, G. P. (1990) *Science* 249, 386–90.
- Wang, B., Dickinson, L. A., Koivunen, E., Ruoslahti, E., and Kohwi-Shigematsu, T. (1995) *J. Biol. Chem.* 270, 23239–42.
- Koivunen, E., Wang, B., and Ruoslahti, E. (1994) *J. Cell Biol.* 124, 373–80.
- Koivunen, E., Wang, B., and Ruoslahti, E. (1995) *Bio/Technology* 13, 265–70.
- Koivunen, E., Gay, D. A., and Ruoslahti, E. (1993) *J. Biol. Chem.* 268, 20205–10.
- Morla, A., and Ruoslahti, E. (1992) *J. Cell Biol.* 118, 421–9.
- Dent, P., Jelinek, T., Morrison, D. K., Weber, M. J., and Sturgill, T. W. (1995) *Science* 268, 1902–6.
- Xiao, B., Smerdon, S. J., Jones, D. H., Dodson, G. G., Soneji, Y., Aitken, A., and Gamblin, S. J. (1995) *Nature* 376, 188–91.
- Garcia-Guzman, M., Dolfi, F., Russello, M., and Vuori, K. (1999) *J. Biol. Chem.* 274, 5762–8.
- Williams, N. G., and Roberts, T. M. (1994) *Cancer Metastasis Rev.* 13, 105–16.
- Tzivion, G., Luo, Z., and Avruch, J. (1998) *Nature* 394, 88–92.
- Zhang, Z., Morla, A. O., Vuori, K., Bauer, J. S., Juliano, R. L., and Ruoslahti, E. (1993) *J. Cell Biol.* 122, 235–42.
- Zhang, L., Chen, J., and Fu, H. (1999) *Proc. Natl. Acad. Sci. U.S.A.* 96, 8511–5.
- Zhang, L., Wang, H., Maters, S. C., Wang, B., Barbieri, J. T., and Fu, H. (1999) *Biochemistry* 38, 12159–64.

BI991353H